ICJK
Journal of Geo-Energy and Environment
http://dx.doi.org/10.62762/JGEE.2025.600070

RESEARCH ARTICLE

Geological Characteristics and Three-Dimensional Development Potential of Deep Shale Gas in the Luzhou Area, Southern Sichuan Basin, China

Jing Li[1], Tingting Huang[1], Hu Li[2,3,*], Xin Gong[1], Zhi Gao[1] and Ang Luo[1]

[1] Institute of Geological Exploration and Development of CNPC Chuanqing Drilling Engineering Company Limited, Chengdu 610051, China
[2] Sichuan University of Science and Engineering, Yibin 644000, China
[3] State Key Laboratory of Oil and Gas Reservoir Geology and Exploitation, Chengdu University of Technology, Chengdu 610059, China

Abstract

Deep shale sedimentary environment, diagenesis, and pore evolution are closely related to the occurrence state and content of shale gas, exerting significant control on reservoir quality. In this study, scanning electron microscopy (SEM), mineral composition, spectral gamma-ray logging, elemental logging, and comprehensive well log data were used to analyze the sedimentary environment. Combined with pore structure and storage space experiments, the geological conditions for deep shale gas accumulation were discussed. The Longmaxi Formation high-quality shale reservoirs in southern Sichuan (Luzhou area) are laterally extensive, vertically thick, and contain well-developed natural fractures; thus, reasonable well pattern deployment is crucial to avoid casing deformation, mitigate fracture interference, and improve productivity. Results show that shale gas enrichment and accumulation are controlled by four main factors: (1) Deep-water anoxic deposition enriching organic matter ("source control"), (2) Source–reservoir coupling controlling accumulation, (3) Temperature–pressure coupling controlling gas content, and (4) Faults controlling preservation. Based on static reservoir characteristics and production dynamics, a three-dimensional inter-well development model was established. Horizontal well spacing is 300–400 m, vertically targeting two layers (Long 1-11 and upper Long 1-13 sublayers) with staggered hydraulic fracturing and phased production. Field statistics show that this multi-layer phased scheme reduces engineering problems, lowers casing deformation incidence, and increases average EUR per 1000 m by about 10% compared with conventional single-layer deployment.

Keywords: deep shale, exploration potential, sedimentary environment, accumulation conditions, Luzhou area.

Submitted: 10 August 2025
Accepted: 22 August 2025
Published: 31 August 2025

Vol. 1, **No.** 1, 2025.
10.62762/JGEE.2025.600070

***Corresponding author:**
✉ Hu Li
lihu860628@126.com, lihu@suse.edu.cn

Citation
Li, J., Huang, T., Li, H., Gong, X., Gao, Z., & Luo, A. (2025). Geological Characteristics and Three-Dimensional Development Potential of Deep Shale Gas in the Luzhou Area, Southern Sichuan Basin, China. *Journal of Geo-Energy and Environment*, 1(1), 32–45.

© 2025 by the Authors. Published by Institute of Central Computation and Knowledge. This is an open access article under the CC BY license (https://creativecommons.org/licenses/by/4.0/).

1 Introduction

Shale gas exploration in the Sichuan Basin has historically focused on marine shales shallower than 3500 m, and China's shale gas production in 2022 reached 24.0×10^8 m^3. Deep shale gas is considered a resource with great potential for enhancing quality and efficiency and achieving strategic production increases; its efficient development is of great significance for advancing China's shale gas industry and realizing the "Dual Carbon" goals [1]. China defines "deep" as 3500–4500 m and "ultra-deep" as deeper than 4500 m. Sun et al. [2]. analyzed the challenges to large-scale efficient development of deep shale gas in the Sichuan Basin and proposed three counterstrategies for achieving effective development. Zhang et al. [3]. reviewed the exploration and development progress of deep shale gas in Weirong and Yongchuan areas, noting that deep shale gas exploitation will require prolonged theoretical and engineering innovations and a step-by-step approach. He et al. [4]. analyzed new progress and challenges in deep shale gas exploration and development in southern Sichuan, concluding that core technologies suited to deep shale conditions in southern Sichuan have basically formed, bolstering confidence in future deep shale gas development. In recent years, with intensified shale gas exploration and development, PetroChina has accelerated the rapid production build-up of shale gas in southern Sichuan. In the central Luzhou area, the Wufeng–Longmaxi formations (Upper Ordovician Wufeng Formation and Lower Silurian Longmaxi Formation) are characterized by a laterally extensive deep-water shelf facies with thick, widespread organic-rich black shale [5]. Data from 11 recently completed appraisal wells (as of 2023) show that the thickness of continuous Class I reservoir is 14–20 m, with favorable reservoir parameters such as high brittle mineral content, good porosity, and high gas saturation, indicating enormous development potential. In the northern part of the Luzhou area, efforts have focused on controlling complex drilling/fracturing issues and increasing single-well production through research and field trials in development policies, drilling, and fracturing techniques, yielding initial results in mechanism understanding and mitigation measures.

However, since large-scale production from the Longmaxi Formation deep shale gas in the Luzhou area, issues such as wellbore casing deformation and inter-well pressure communication (fracture hits) have gradually emerged, becoming major factors affecting the profitable development of middle-to-deep shale gas. Recognizing that shale gas reservoirs are essentially man-made and that the geologic system has a safety threshold for pressure, earlier researchers explored measures like limiting total fracturing fluid volume in an area, controlling injection rates, differential fracturing design, and precise execution [6]. These approaches have effectively curbed severe casing deformation and strong inter-well pressure interference, but have not completely solved the problems. Implementing a three-dimensional (multi-layer) well deployment (often called stereoscopic development) among wells is a bold attempt to prevent such complex issues. By continually refining the understanding of the geological and engineering characteristics in the Luzhou area, an approach of phased fracturing and phased production was adopted to alter the in-situ stress state and eliminate severe casing deformation [7]. Additionally, three-dimensional (vertical staggered) development was employed to prevent intense inter-well fracture communication while also enhancing the degree of reserves utilization, effectively integrating well placement strategy into the complexity mitigation measures.

In order to clarify the geological characteristics of high-quality deep shale gas reservoirs and assess their three-dimensional development potential, this paper analyzes the sedimentary environment of the deep shale using SEM observation and mineral composition analysis, together with spectral log, elemental log, and comprehensive logging data. We then integrate reservoir pore structure characteristics and pore space features from laboratory analyses to discuss the enrichment characteristics and accumulation conditions of deep shale gas. Finally, based on the static reservoir attributes of the Longmaxi Formation shale and the dynamic production performance in the study area, we evaluate an inter-well three-dimensional development well pattern for the main production zone in the northern Luzhou area and assess its effectiveness.

2 Geological Setting

The study area is structurally situated in a transitional zone influenced by major fault systems. It is bounded by the Huaying Mountain fault to the west and the Qijiang fault to the east, and is constrained by the Changyuanba structure to the south, collectively forming an overall triangular structural area that belongs to a complex multi-structural

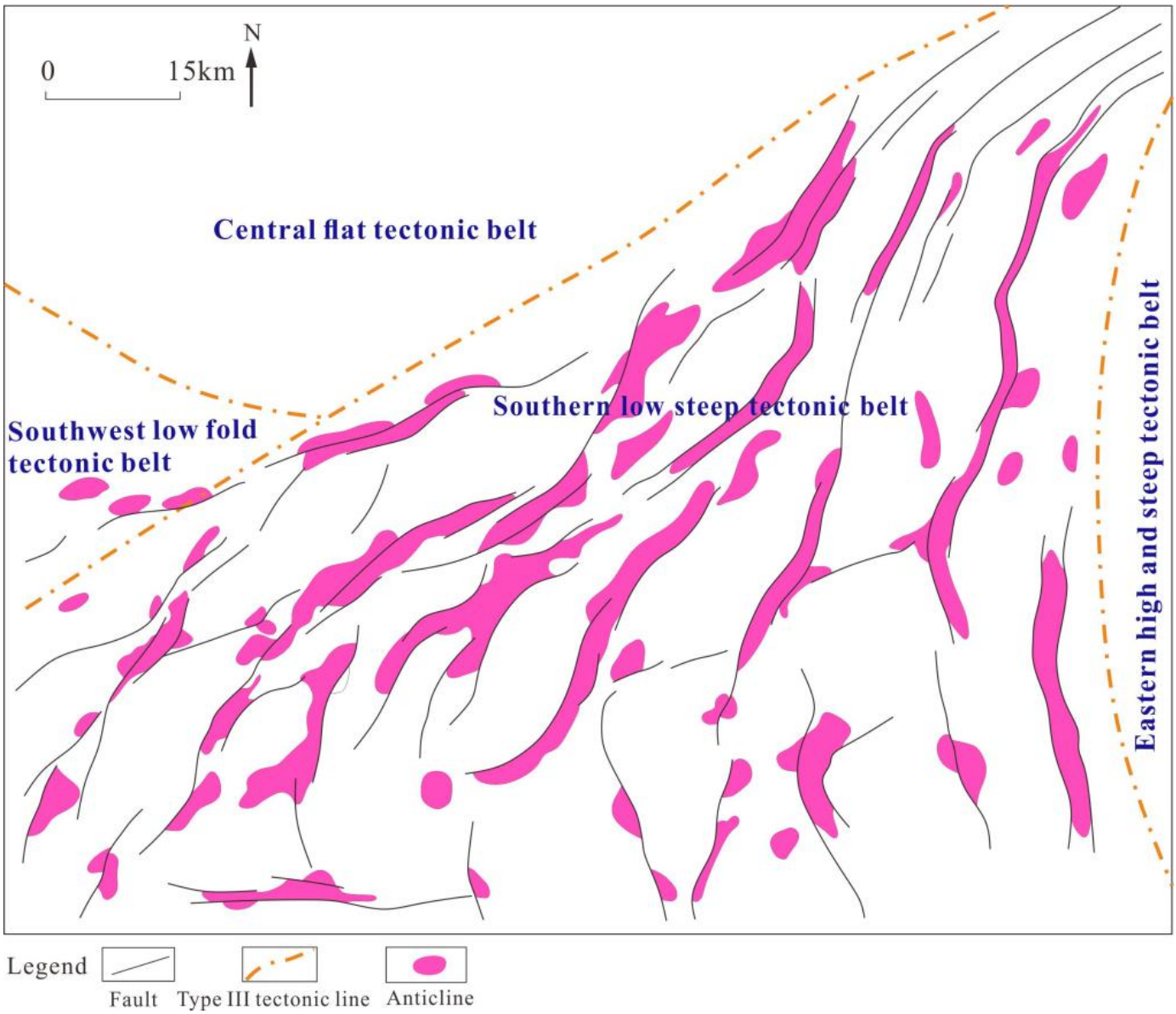

Figure 1. Tectonic fault distribution in the central Luzhou area of southern Sichuan Basin.

transition system [8]. The central part of the Luzhou area lies mainly in the southern Sichuan low-relief tectonic belt. Based on structural style and fault systems, the area corresponds to a second-order structural unit defined as the northern Luzhou "broom-shaped" structure, and third-order units including the Fujie syncline, Desheng-Baozang syncline, and Laishu-Yunjin syncline. Overall, the folding intensity in the central block is weaker than that in the northern Luzhou area. The central Luzhou area inherited the "low-amplitude anticline alternating with broad gentle syncline" structural pattern characteristic of northern Luzhou, but with even more developed minor structures and small faults. Within the block, no first-order (major) faults cut the Wufeng Formation basal boundary. The second-order faults, after passing through the central transfer zone, change orientation to some extent. More numerous third- and fourth-order small faults are developed inside the synclines, with three dominant strike sets observed: NE–SW, N–S, and E–W (as shown in Figure 1) [9].

The study area forms a triangular structural zone bounded by major faults, and contains numerous small-scale faults. The map highlights the regional tectonic belts, including the central low-relief (flat) tectonic belt, the southwestern low-fold belt, the southern low-steep belt, and the eastern high-steep tectonic belt. Pink areas denote anticlines, black lines are major faults, and orange dashed lines are minor (Type III) tectonic lines (fold axes).

3 Deep Shale Reservoir Characteristics Evaluation

3.1 Organic matter content and thermal maturity

In the central Luzhou area, the lower Longmaxi Formation (Long 1 member) is subdivided into multiple sublayers. Geochemical analysis shows that the total organic carbon (TOC) content is relatively high in these deep shales (all in over-mature thermal stage). For example, in sublayer Long 1-11, TOC ranges from 4.5% to 6.1%, with an average of 5.5%. In Long 1-12, TOC ranges 3.4–4.8% (avg. 4.3%), and in Long 1-13, 2.7–4.7% (avg. 3.8%). Thus, sublayer Long 1-11 has the highest organic carbon content, followed by Long 1-12, and Long 1-13 slightly lower. In individual wells, the organic matter content is consistently high. For example, well L12 shows TOC of 4.6–6.0% (avg. 4.8%) across sublayers Long 1-11 to Long 1-13; well L18 shows 4.1–5.4% (avg. 4.6%); and well L19 shows 4.1–5.6% (avg. 4.4%) in the same interval. Spatially, the TOC of sublayers Long 1-11 through Long 1-12 is generally between 4.0% and 5.0% across most of the study area. Higher TOC ($>$ 5.0%) is observed in the northern and central parts of the block, while values gradually decrease southward, reaching around 4.5% in the southernmost well L26 area. During the Long 1-11 to Long 1-13 sublayer deposition, most of the region had TOC between 4.0% and 5.0%, with the northern area slightly higher ($\sim$ 4.8%) and a gradual reduction toward the south ($\sim$ 4.0%). This distribution reflects the depositional environment and organic productivity variations across the block (as shown in Figure 2(a).

3.2 Mineral composition and brittleness

The mineralogical composition of the deep shales in central Luzhou is dominated by brittle minerals (primarily quartz, feldspar, and carbonates) with lesser clay, contributing to high brittleness—an important factor for hydraulic fracturing [10]. In sublayer Long 1-11, the brittle mineral content ranges from 72.4% to 88.4% (average 81.1%). Sublayer Long 1-12 is similar, 72.0–88.8% (avg. 81.1%). Sublayer Long 1-13 is slightly lower, 62.1–72.3% (avg. 66.8%). Thus, Long 1-11 and Long 1-12 have the highest brittle mineral percentages, whereas Long 1-13 is comparatively lower. Overall, across Long 1-11 and Long 1-12, the shale brittle mineral content is typically $>$ 73%, and considering Long 1-11 through Long 1-13 together, it ranges mostly between 69% and 83%. For instance, well L12 has 64.0–84.8% brittle minerals (avg. 78.2%) in sublayers Long 1-11–1_3; well L18 has 66.6–80.5% (avg. 72.8%); and well L19 has 63.9–74.3% (avg. 69.3%). In map view, the brittle mineral content of sublayers Long 1-11 and Long 1-12 exceeds 70% nearly everywhere, with the highest values ($\sim$ 88%) in the southern part of the area. The content then gradually decreases toward the central part ($\sim$ 82%) and further to the northwest ($\sim$ 74%). Considering the entire Long 1-11 to Long 1-13 interval, the brittle mineral content shows a southwest-to-northeast decreasing trend: e.g., around well L26 in the southwest a high of $\sim$ 82% is observed, dropping to $\sim$ 69% near well L19 in the northeast (as shown in Figure 2b).

3.3 Pore development characteristics

Porosity in the deep shale is modest but non-negligible, given the considerable burial depth ($\sim$ 4 km). Measured porosity values in central Luzhou for sublayer Long 1-11 range from 4.4% to 7.7% (avg. 5.9%); Long 1-12 from 4.3% to 6.9% (avg. 5.3%); and Long 1-13 from 5.4% to 7.8% (avg. 6.5%). Interestingly, Long 1-13 shows the highest average porosity among these, slightly higher than Long 1-11, while Long 1-12 is the lowest. Combining sublayers, Long 1-11 and Long 1-12 generally have porosities between $\sim$ 4.4% and 7.1%, and the range across Long 1-11 to 1-13 is 4.7–7.4%. In specific wells, porosity follows the regional trends: well L12 has 4.9–6.3% (avg. 5.3%) across sublayers Long 1-11–1_3; well L18, which is in the northeast of the area, has higher values 6.9–7.6% (avg. 7.3%); and well L19 also in the NE has 6.9–7.8% (avg. 7.4%). In map view, sublayers Long 1-11 and Long 1-12 both show a decline in porosity from the northeast toward the southwest. The highest porosities ($\sim$ 7.0%) are around wells L18–L19 in the NE, decreasing to $\sim$ 4.9% near well L26 in the far south/southwest. Over the entire Long 1-11 to 1-13 interval, porosity ranges from $\sim$ 4.9% to 7.4%, with a high zone of $\sim$ 7.2–7.4% in the northeast (L18–L19 area), $\sim$ 6.7% in the central area (well L14), and gradually dropping to $\sim$ 4.9–5.0% toward the southwest (well L24 and beyond) (as shown in Figure 2(c)). These porosity values, while lower than those of shallower shale reservoirs, are relatively high for such deep shales, indicating preservation of pore space due to factors like high brittle mineral content resisting compaction and possibly overpressure.

3.4 Gas content characteristics

Gas content (typically expressed in m^3 of gas per tonne of rock, m^3/t) reflects both the amount of adsorbed gas and free gas in the reservoir. In the central Luzhou

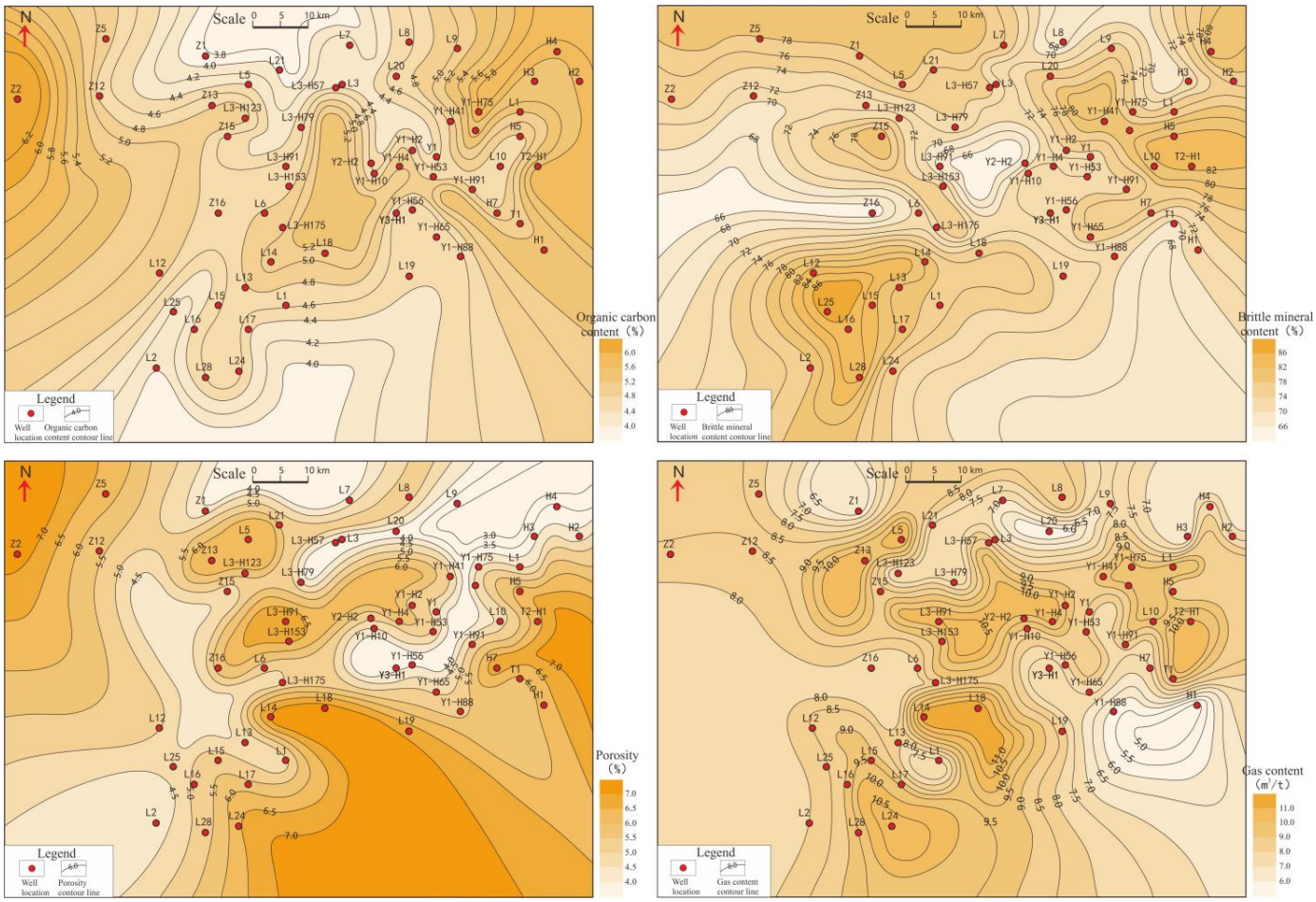

Figure 2. Planar distribution maps of reservoir properties in the central Luzhou area for the Long 1-11 and Long 1-12 shale sublayers. a. TOC content contour map. b. Brittle mineral content contour map. c. Porosity contour map. d. Gas content contour map.

deep shale, gas content is substantial. For sublayer Long 1-11, measured gas content ranges from 8.4 to 13.4 m^3/t, with an average of 10.6 m^3/t. For Long 1-12: 7.0–12.1 m^3/t (avg. 9.1), and Long 1-13: 6.2–12.2 m^3/t (avg. 9.0). Thus, Long 1-11 again exhibits the highest gas content on average, followed by Long 1-12, with Long 1-13 roughly comparable to Long 1-12. Overall, across Long 1-11 and Long 1-12, most gas content values fall in the range 7.5–12.3 m^3/t, and for Long 1-11 through 1-13 collectively in the range 6.9–12.1 m^3/t. Individual well data underscore regional differences: in well L12, the Long 1-11–1_3 interval has 8.4–10.3 m^3/t (avg. 8.7); well L18 in the north shows much higher gas content, 11.8–12.2 m^3/t (avg. 12.1); while well L19 in the northeast has 7.7–10.0 m^3/t (avg. 8.7). Spatially, sublayers Long 1-11 and 1-12 show a trend of higher gas content in the northern part of the area, decreasing outward. For instance, around wells L14–L18 in the north, gas content reaches $\sim$ 12.3 m^3/t, and it tapers off toward the flanks: down to $\sim$ 7.5 m^3/t in the central area near well L1, then rising again slightly to $\sim$ 10.9 m^3/t in the far south near well L24. Over the entire Long 1-11 to 1-13 interval, total gas content ranges from about 6.0 to 12.1 m^3/t. The highest gas contents ($\sim$ 12 m^3/t) occur in the northern wells L14–L18, diminishing in all directions, with a notable low in the central area, and a secondary increase to $\sim$ 10.6 m^3/t at the southeastern edge near well L24 (as shown in Figure 2(d)). The relatively high gas content observed, especially in the north under good preservation conditions, is promising for exploration and production.

4 Deep Shale Gas Enrichment Characteristics and 3D Development Potential Analysis

4.1 Coupled "source-reservoir" conditions controlling accumulation

The type and quality of organic matter (kerogen) fundamentally determine hydrocarbon generation potential. In the Luzhou area, the Wufeng–Longmaxi shale has kerogen predominantly of Type I (with minor Type II_1), indicating the organic matter is

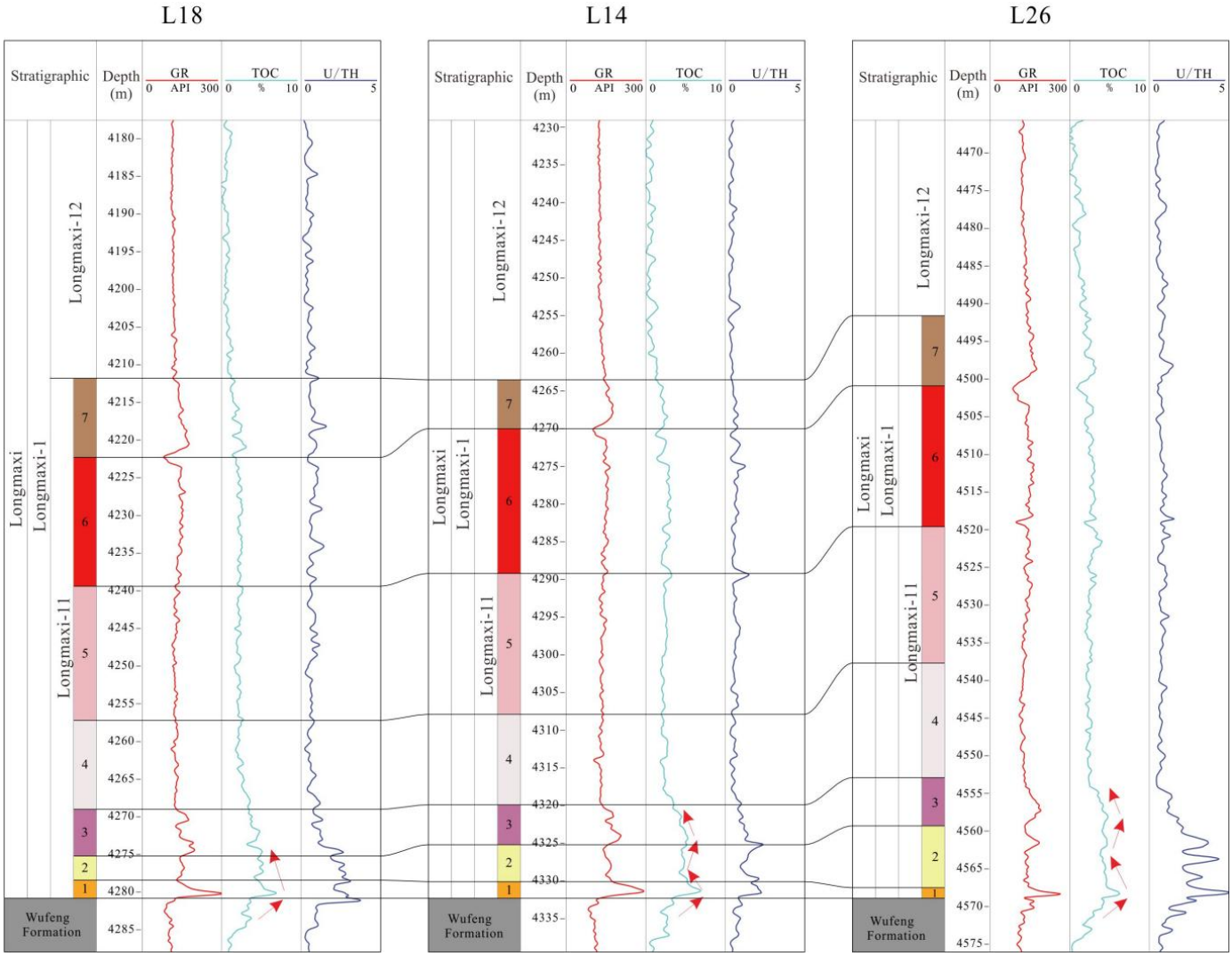

Figure 3. TOC and U/Th well profile of deep shale gas in Luzhou area.

mainly derived from planktonic organisms and algae—an excellent source material with high hydrocarbon-generative potential. The total amount of hydrocarbon generated depends on both TOC content and the thickness of high-quality shale. These factors constitute the material basis for shale gas reservoirs to form. In the study area, the vertical variation of TOC in the Wufeng–Longmaxi shales typically shows a three-segment pattern of "Decrease–Increase–Decrease" from bottom to top (as shown in Figure 3). The basal part of the Longmaxi Formation generally exceeds 60 m of high-quality black shale. For example, in representative wells L18, L14, and L26, the overall TOC of the Wufeng–Longmaxi shale ranges from 0.28% up to 7.5%, with the basal high-quality shale having TOC of 1.9–7.5% (average $\sim$ 3.97%). Within the Long 1 submember, there are distinct TOC peaks at certain horizons (corresponding to sublayers Long 1-11 and Long 1-13 in this area). Geochemical redox proxies further illuminate the depositional environment control: for instance, the U/Th ratio in wells L18, L14, L26 reaches elevated values (U/Th = 3.63, 2.20, 5.08, respectively) in the first sublayer of the Long 1, indicating strongly anoxic bottom-water conditions during deposition of the basal Longmaxi shale. The U/Th then decreases, and rises again to secondary peaks (up to $\sim$ 2.4–2.7) at the top of the second sublayer of Long 1, above which (sublayers 4–7) U/Th falls below 1.5, reflecting more oxygenated conditions. These data suggest that a low-energy, undercompensated, anoxic deep-water shelf setting prevailed during deposition of the organic-rich shales, especially in the basal Longmaxi which corresponds to the highest TOC and is thick (often $>$ 60 m). The combination of high organic productivity/preservation (high TOC), suitable thermal maturity (vitrinite reflectance Ro generally $>$ 3.0 indicating over-mature dry gas stage), and

substantial effective thickness of rich shale ensures a strong hydrocarbon generation supply for the shale gas system. In summary, the coupling of a rich source (abundant Type I kerogen, high TOC, thick organic-rich intervals) with reservoir properties (sufficient porosity and adsorption capacity in the same interval) is a key control on gas accumulation in the deep shale — essentially the "source-reservoir coupling" that determines gas in-place[11].

4.2 Temperature and pressure characteristics

The Longmaxi Formation is deeply buried and exhibits higher formation temperatures than other middle-depth shale gas regions like Changning or Weiyuan [12]. In the northern Luzhou area, bottom-hole temperatures of vertical wells range from $\sim$ 102°C to 132°C (average $\sim$ 121°C). In the central Luzhou area, conventional vertical wells have recorded temperatures of 111–137°C (avg. $\sim$ 128°C), while horizontal well sections reach even higher, 130–163°C (with the highest $\sim$ 163°C in well L16). Such elevated geothermal gradients result in an over-mature thermal regime (Ro $>$ 3.0, dry gas), but also could enhance matrix permeability and gas desorption in some cases. Pressure-wise, the deep shale in this area is characterized by high formation pressures. The pressure coefficient (ratio of formation pressure to hydrostatic pressure) is around 2.2 across the central Luzhou area. This indicates a strongly overpressured system, which is beneficial for gas preservation and productivity as it counteracts gas diffusion. The combination of high temperature and high pressure in the Luzhou deep shale gas indicates that the gas is in a high-energy state. The high pressure is particularly critical for maintaining gas content (as per adsorption isotherms, higher pressure means more gas can be held in the shale). In fact, the coupling of temperature and pressure exerts a control on gas content: higher temperature can reduce adsorption capacity slightly but significantly increases desorption/diffusivity, while high pressure greatly increases gas storage capacity. The net effect in Luzhou is that these deep shales still retain high gas content (as seen in measurements), implying that overpressure is the dominant factor helping retain gas despite high temperatures. Generally, good preservation (minimal leakage) is inferred since pressure coefficients $\sim$ 2.0–2.3 suggest the gas is effectively trapped and not extensively dissipated. Figure 4 illustrates the spatial distribution of geothermal temperature and pressure coefficient in the Luzhou area, showing that the core of the block is both a thermal anomaly and an overpressure cell, favorable for shale gas enrichment.

4.3 Influence of faults on shale gas preservation

Fault can significantly impact shale gas preservation by providing pathways for gas escape or, conversely, by compartmentalizing pressure if sealed [13]. In the central Luzhou area, Formation Micro-Imager (FMI) logs reveal that most wells exhibit a network of natural fractures, predominantly with two strike sets: NW–SE (around $330° \pm 10°$) and NE–SW ($30° \pm 5°$), followed by W–E ($90° \pm 5°$). For example, in the L14 well area, fractures are mainly NW ($\sim 340°$) and NEE ($\sim 60°$) trending, with minor NNE ($\sim 10°$) and near-EW sets. The L15 well area also shows a fracture network with major sets at NEE ($\sim 60°$), NWW ($\sim 330°$), and another NEE ($\sim 50°$) set, plus an EW set. In L26, the dominant fractures are NEE ($\sim 70°$) and EW ($\sim 90°$), with secondary NNE ($\sim 10°$). Most of these fractures are high-angle to near-vertical (dip angles 30°–80°, commonly $> 60°$), which aligns with core observations. A histogram of fracture dip angles in the study area shows a predominance of steeply dipping and near-vertical fractures, with very few low-angle or bedding-parallel fractures (indicating that horizontal fractures are scarce). These high-angle fractures are likely related to multiple tectonic events (as shown in Figure 5) [14].

Structurally, as mentioned, the Luzhou central block continues the low-relief anticline pattern of the north but with more numerous small faults. There are essentially no through-going major faults in the target interval, only smaller-scale faults of various orientations. Fault timing analysis indicates that the maximum horizontal principal stress ($S_{H_{\max}}$) during different tectonic stages influenced fault sealing [15]. Early-stage (late Yanshanian, Cretaceous) saw formation of W-E to NEE trending faults (Phase I) due to regional extension (gravity sliding along the underlying Cambrian ductile layer). These early Phase I fractures formed early and often became mineral-filled, thus their impact on present gas leakage is minimal (they are largely sealed). In the early to mid Himalayan (69–46 Ma), uplift of the Qinghai-Tibet plateau caused NW-directed compression in this region, generating NE-trending faults (Phase II). These NE faults vary in size and distribution and can detrimentally affect shale gas preservation. Along the NE faults, oblique shear under SE–NW stress caused some transtensional openings, meaning larger NE-oriented faults tend to be less sealing and can act as leakage pathways. Finally, in the late Himalayan

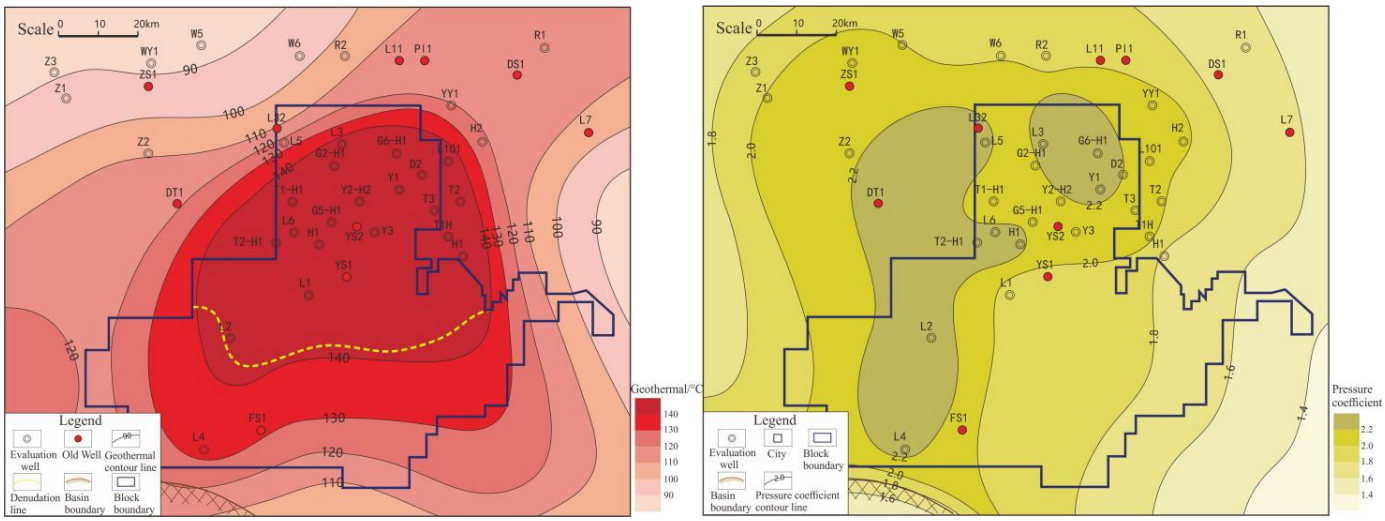

Figure 4. Maps of formation temperature (left) and pressure (right) in the Luzhou area.

(Miocene to present, $\sim$ 30–0 Ma), the influence of the Jiangnan Xiuwu uplift imposed nearly E–W compression, forming N–S (to NNW/SSE) trending faults (Phase III). These Phase III near-SN faults under the current stress regime ($SH_{\max} \sim 105° \pm 5°$) are oriented at a high angle to the stress, meaning they are more compressional (closing) in nature and likely have good sealing capacity. In summary, faults of different orientations have different effects: the larger NE-trending faults (Phase II) present in the area are the most likely to compromise gas preservation because they experienced strike-slip and extensional components that kept them more open. Small- to medium-scale faults that are favorably oriented (large angle) to the present stress tend to remain closed and thus have limited impact on gas retention. Overall, shale gas is best preserved in zones where faults are minor or sealed. The Luzhou deep shale gas play benefits from the fact that no large through-going faults cut the reservoir; the faults present are relatively small scale and many have good sealing due to mineral fill or current stress orientation. Particularly, fractures with significant misalignment ($> 20°$) from the present maximum stress (such as NWW, NNE, NEE sets) can actually enhance gas retention by increasing fracture closure, and moderate fracture development can even improve storage (by creating secondary porosity) without causing leakage. Figure 5 shows examples of FMI log fracture interpretations and their orientations, as well as rose diagrams and frequency histograms of fracture strikes for both high-conductivity (open) and high-resistivity (sealed) fractures. It can be seen that high-conductivity (potentially open) fractures are predominantly NW and NE oriented (red and blue roses), whereas many of the other orientations correspond to filled fractures (yellow roses) that are likely sealed. This interplay of fracture orientation and sealing status is a critical factor in the gas preservation of the deep shale (as shown in Figure 6).

4.4 Three-dimensional development potential analysis

A well-planned well spacing and vertical stacking strategy, combined with an optimized hydraulic fracturing program, can greatly improve shale gas recovery. Operators in China and abroad typically use methods such as fracturing simulation, numerical reservoir simulation, and field pilots to determine optimal well spacing and well patterns [16]. In shale gas development, the concept of "closer well spacing with dense well networks" has become mainstream for maximizing reservoir contact. However, drilling too many wells in the same layer with overly small inter-well spacing can lead to severe fracture interference (pressure communication) and strong inter-well competition during production. An alternative approach is 3D development, which involves deploying wells in multiple stratigraphic layers (a stacked or staggered well pattern) to increase the volume of reservoir stimulated in both lateral and vertical dimensions. A 3D well pattern can enhance the utilization of geological reserves in different layers, while also alleviating inter-well pressure interference by separating fracture networks vertically [17]. The core issue in designing a shale gas well pattern is balancing well spacing with the effective fracture half-length achieved by stimulation—essentially optimizing the match between well density and fracture geometry.

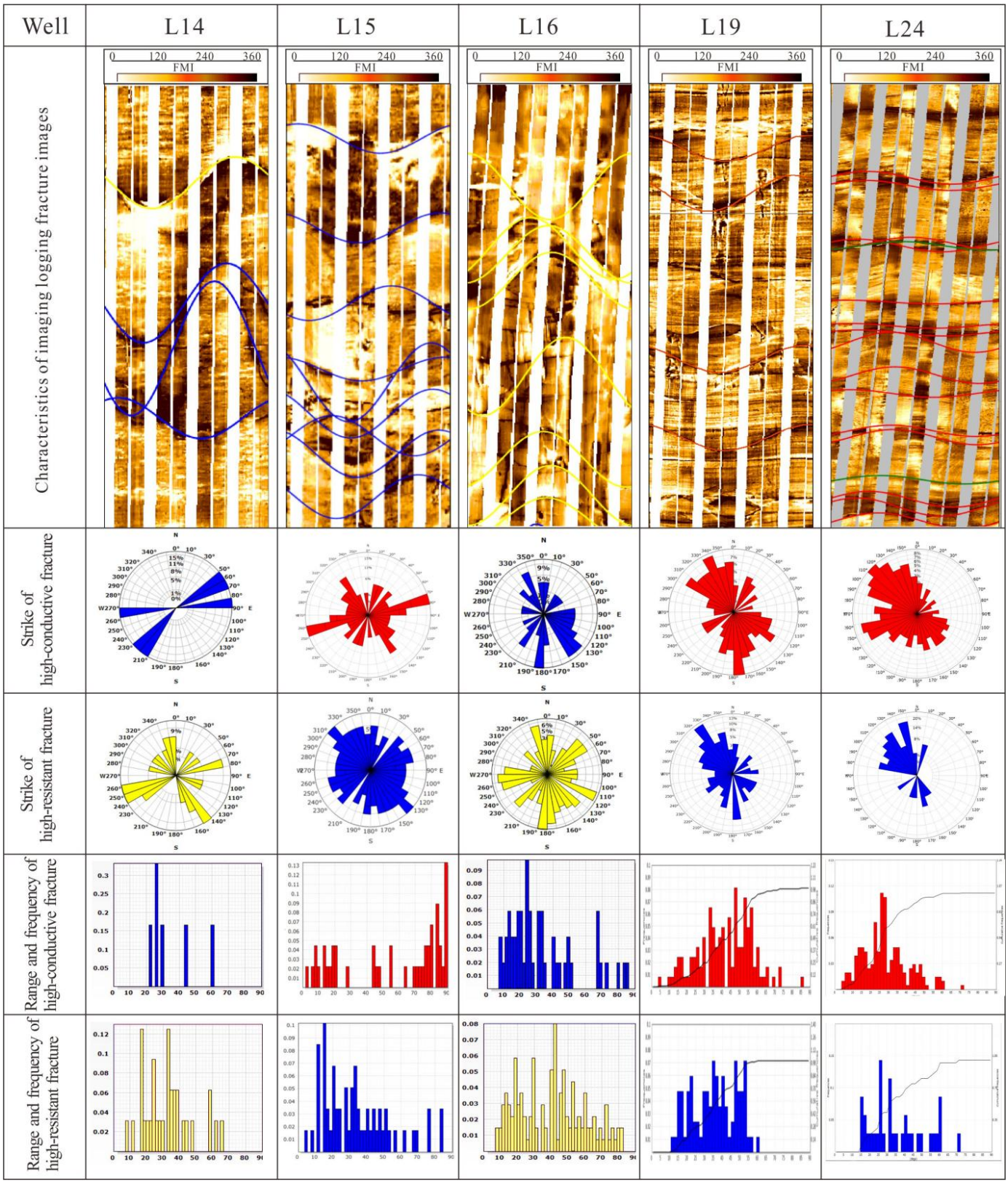

Figure 5. Characteristics of natural fractures from FMI in representative wells (L14, L15, L16, L19, L24) in the Luzhou area, and their orientation statistics.

Within the Longmaxi Formation, the upper submember exhibits excellent reservoir qualities and is considered highly promising for multi-layer development. Detailed sedimentological and log analysis allowed further subdivision the fourth sub-member into four smaller units: Long 1-14, 1-15, 1-16, and 1-17 sublayers. These subdivisions are based on slight lithofacies differences and marker

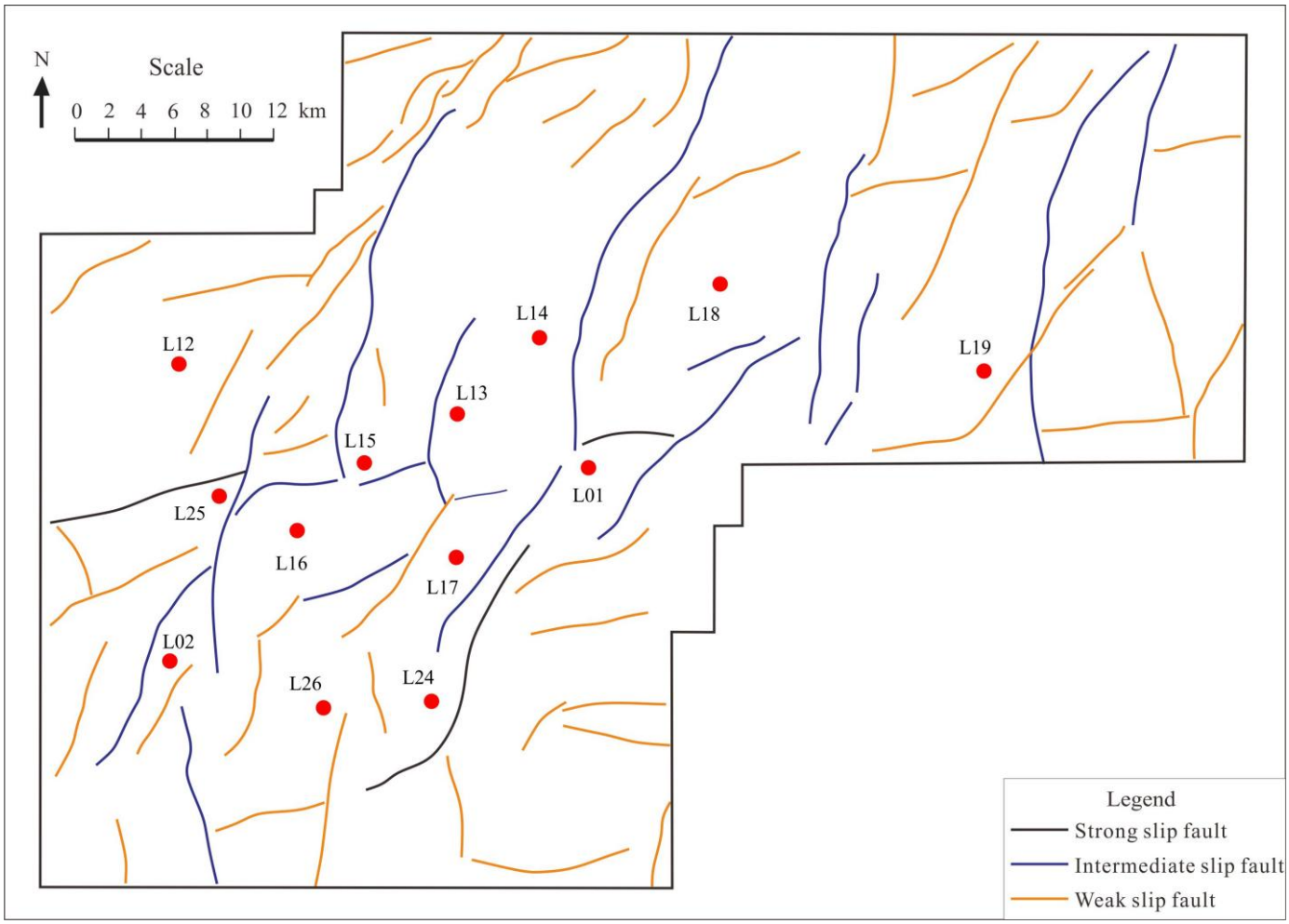

Figure 6. Fault characteristic of deep shale gas in Luzhou area.

beds recognizable on logs: for example, the top of Long 1-14 sublayer commonly contains a thin silty shale, and the top of Long 1-16 sublayer contains a thin calcareous shale, both representing distinct lithologic interfaces. The depositional environment throughout Long 1-14 to Long 1-17 was a low-energy, underfilled (sediment-starved) deep-water setting with bottom-water anoxia—conditions favorable for accumulating organic-rich shale [18]. Notably, within this upper interval, sublayers Long 1-14 and Long 1-16 correspond to relatively deeper-water episodes and show the most favorable reservoir parameters among the set. Focusing on a pilot development area (wells L201–L202), the cumulative thickness of Class I + II reservoir in these upper sublayers is 35–40 m (slightly thinner than in the northern Luzhou area where it is 30–50 m). The contiguous thickness of Class I reservoir alone in the upper interval is generally 1–5 m; at well Lu218 in central Luzhou it reaches 4–5 m, which is the thickest, and overall the thickness trends mirror those of the combined I+II reservoir (thicker in north, thinning south). Importantly, reservoir quality in these upper sublayers is consistently good across layers and the lateral variability is small—meaning each sublayer (Long 1-14 through Long 1-17) is laterally continuous and has similar high quality, and there is clear separation between layers. The contribution of these upper sublayers to well production has been significant in tests, suggesting strong potential for staggered (multi-layer) development in the vertical sense. In other words, because the upper sublayers all yield high gas rates and are separated by identifiable thin barriers, there is an opportunity to develop them in a staggered fashion (one above the other) to increase overall recovery.

On the other hand, one must consider fracture connectivity between layers. Some natural fractures in the field are "through-going" (vertically extensive) and, if intersected by wellbores at large angles, can cause inter-well pressure communication (frac hits) across layers [19]. In comparison to a single-layer dense pattern, a 3D staggered pattern must ensure that vertical fracture networks from different layers

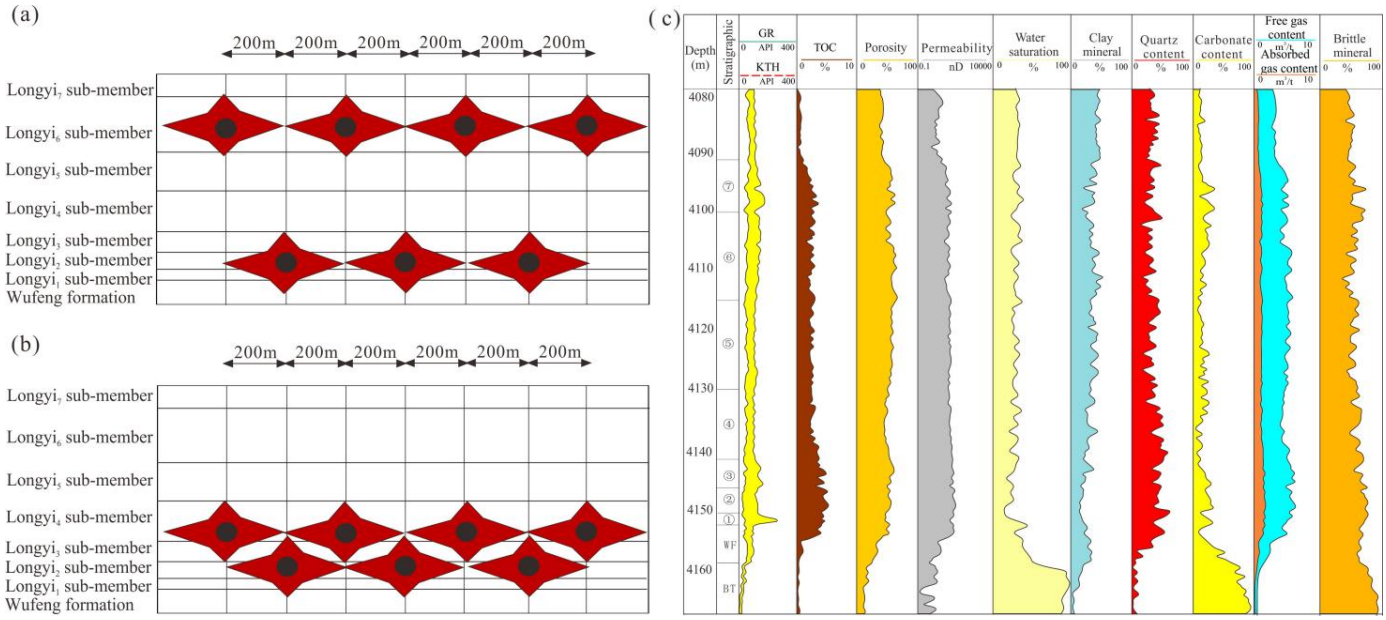

Figure 7. Schematic of 3D development well patterns ("W-type" well arrangements) and target layer selection in the Luzhou area. a. W-pattern Type I. b. W-pattern Type II. c. Comprehensive stratigraphic column.

do not excessively overlap. If overlapping (especially in presence of through-going natural fractures), the risk of inter-layer interference increases. Achieving true volumetric stimulation is more challenging in a multi-layer context and may require a slightly larger horizontal well spacing to accommodate separate fracture networks. Therefore, to balance resource utilization, single-well EUR, and engineering risks, it may be advisable to space wells a bit farther apart when employing multi-layer (3D) development than one would in a single-layer dense pattern. This ensures each well's fracture network can develop fully without merging prematurely with that of another well. In summary, the upper Longmaxi sublayers offer high-quality targets for 3D development, but well spacing and fracturing parameters need to be optimized to account for natural fracture systems. A conceptual "W-shaped" well configuration (described below) has been proposed to exploit these layers, and initial trials suggest promising results, though further validation is ongoing in areas with through-going fractures [19, 20].

A "W-type" well pattern refers to a specific multi-layer well deployment scheme where wells targeting an upper layer and wells targeting a lower layer are interlaced in plan view, resembling the letter "W" when connecting wellbores in cross-section. In the Luzhou area, two variants of the W-pattern have been designed for 3D development. Pattern I places the upper-layer horizontal wells in sublayer Long 1-16, and the lower-layer horizontal wells in the basal Long 1-12 sublayers. The vertical separation between the two sets of wells is about 40 m. Pattern II places the upper-layer wells in sublayer Long 1-14 (specifically near its base, about 5 m above that boundary) and the lower-layer again in Long 1-12; here the vertical separation is only about 10 m. Both patterns aim to increase stimulated reservoir volume, but their interference characteristics differ. In Pattern I, the upper well's target (Long 1-16) is sufficiently far above the lower target (Long 1-1/1-2) that their induced fracture networks do not significantly interact vertically; there is minimal overlapping of the stimulated zones, yielding a larger overall effective fractured volume. This is expected to result in a higher cumulative gas production per well pair. In Pattern II, however, the upper target (Long 1-14) is much closer to the lower target, so fractures are more likely to overlap or interact, creating some redundancy in stimulated volume and a relatively smaller total fractured volume. Consequently, the predicted cumulative production for Pattern II is lower than Pattern I, although within Pattern II small variations in vertical spacing did not show large differences in outcome.

For the Luzhou area conditions, the recommended W-pattern is to use sublayer Long 1-1112 (lower part of Long 1 member) as the lower target, and sublayer Long 1-16 (upper part of Long 1 member) as the upper target. The reservoir properties of these chosen target layers are favorable: in the lower target (Long 1-1112 interval), the porosity is ~5%, total gas content ~8.4-9.0 m^3/t, brittle mineral content 70-75%, TOC

~4.8-5.5%, and gas saturation ~68-70%. In the upper target (Long 1-16 sublayer), porosity is ~5%, gas content ~7.5 m^3/t, brittle mineral ~69%, TOC ~4.6%, and gas saturation ~58%. Thus, both layers have high brittleness and decent porosity/gas content, though the lower layer holds somewhat more gas (due to higher pressure and saturation). The W-pattern well arrangement essentially involves two horizontal wells vertically spaced, one in each target layer, with their surface locations offset such that the laterals are not directly above one another but staggered (hence the "W" shape when connecting the dots). This approach maximizes coverage while preventing overlapping fractures.

Preliminary field implementations of the W-type 3D development in the Luzhou area indicate that when through-going natural fractures are present, the multi-layer "W" well configuration can still face challenges, and its effectiveness needs further verification under different well spacing and fracturing parameters. Ongoing tests aim to calibrate the optimal horizontal spacing for W-pattern wells to ensure minimal frac hits between the upper and lower wells. Nevertheless, early results are encouraging: the wells in the multi-layer pattern are achieving better productivity than conventional single-layer patterns, and the engineering complications (like casing deformation and inter-well interference) have been manageable when the design is done carefully. Figure 7 illustrates the W-type well pattern designs and a comprehensive log section of a typical well that highlights the target sublayers and their properties.

5 Conclusions

(1) The deep shale gas in the Luzhou area is controlled by four main enrichment factors: (a) Deep-water anoxic depositional environments that control organic matter enrichment ("source control"); (b) The coupling of source and reservoir conditions that controls gas accumulation; (c) Temperature–pressure coupling that controls gas content; and (d) The fault that controls shale gas preservation conditions.

(2) The Longmaxi Formation high-quality shale reservoirs in the southern Sichuan Luzhou area are laterally extensive and continuous, have large vertical thickness, and contain well-developed natural fractures. A reasonable well pattern deployment is of great importance for preventing gas well casing deformation, mitigating inter-well fracture interference, and improving well productivity.

(3) Based on the static reservoir characteristics and production dynamics of the Longmaxi Formation shale in the study area, a three-dimensional (multi-layer) inter-well development model was analyzed for the main production zone. In this model, the horizontal well spacing is 300–400 m, and vertically it targets two layers (the Long 1-11 sublayer and the upper portion of the Long 1-13 sublayer) with staggered hydraulic fracturing and phased production. Field statistics indicate that the phased, multi-layer development scheme can effectively mitigate complex engineering problems, reduce the incidence of casing deformation, and increase the average EUR (estimated ultimate recovery) per 1000 m of lateral length by about 10% compared to a conventional single-layer well deployment.

Data Availability Statement

Data will be made available on request.

Funding

This work was supported in part by the National Natural Science Foundation of China under Grant 42102167 and the Science and Technology Cooperation Project of the CNPC-SWPU Innovation Alliance under Grant 2020CX020000; in part by the State Key Laboratory of Oil and Gas Reservoir Geology and Exploitation under Grant CDUT-PLC2025011 and Grant PLN2023-31.

Conflicts of Interest

Jing Li, Tingting Huang, Xin Gong, Zhi Gao and Ang Luo are affiliated with the Institute of Geological Exploration and Development of CNPC Chuanqing Drilling Engineering Company Limited, Chengdu 610051, China. The authors declare that this affiliation had no influence on the study design, data collection, analysis, interpretation, or the decision to publish. Hu Li served as an Editor-in-Chief of the *Journal of Geo-Energy and Environment* at the time of manuscript submission. To ensure the integrity of the peer-review process, Hu Li was not involved in the editorial handling, peer review, or decision-making process for this manuscript, which was handled independently by another editor. The remaining authors declare no conflicts of interest.

Ethical Approval and Consent to Participate

Not applicable.

References

[1] Wu, M., Xiong, Y., Qin, Y., & Peng, J. (2025). Brief Analysis of Intelligent Collaborative Management of Oil and Gas Field Enterprises under the" Dual Carbon" Goals: Based on the Integration and Innovation of Green Low-Carbon and Digital Technologies. *Frontiers in Economics and Management, 6*(6), 20-26. [Crossref]

[2] Sun, C., Nie, H., Dang, W., Chen, Q., Zhang, G., Li, W., & Lu, Z. (2021). Shale gas exploration and development in China: Current status, geological challenges, and future directions. *Energy & Fuels, 35*(8), 6359-6379. [Crossref]

[3] Zhang, L., He, X., Li, X., Li, K., He, J., Zhang, Z., ... & Liu, W. (2022). Shale gas exploration and development in the Sichuan Basin: Progress, challenge and countermeasures. *Natural Gas Industry B, 9*(2), 176-186. [Crossref]

[4] He, X., Chen, G., Wu, J., Liu, Y., Wu, S., Zhang, J., & Zhang, X. (2023). Deep shale gas exploration and development in the southern Sichuan Basin: New progress and challenges. *Natural Gas Industry B, 10*(1), 32-43. [Crossref]

[5] Fan, C., Li, H., Qin, Q., He, S., & Zhong, C. (2020). Geological conditions and exploration potential of shale gas reservoir in Wufeng and Longmaxi Formation of southeastern Sichuan Basin, China. *Journal of Petroleum Science and Engineering, 191*, 107138. [Crossref]

[6] Shen, C., Wu, J., Zeng, B., Song, Y., Yao, Z., Dong, Y., & Du, Y. (2024). Measures and results of prevention and control on casing deformation and frac-hit in deep shale gas wells in Southern Sichuan Basin. *Natural Gas Industry B, 11*(3), 262-273. [Crossref]

[7] Xu, Z., Liang, X., Lu, H., Zhang, J., Shu, H., Xu, Y., ... & Shi, W. (2020). Structural deformation characteristics and shale gas preservation conditions in the Zhaotong National Shale Gas Demonstration Area along the southern margin of the Sichuan Basin. *Natural Gas Industry B, 7*(3), 224-233. [Crossref]

[8] Li, J., Li, H., Yang, C., Wu, Y., Gao, Z., & Jiang, S. (2022). Geological characteristics and controlling factors of deep shale gas enrichment of the Wufeng-Longmaxi Formation in the southern Sichuan Basin, China. *Lithosphere, 2022*(Special 12), 4737801. [Crossref]

[9] Yong, R., Chen, G., Yang, X., Huang, S., Li, B., Zheng, M., ... & He, Y. (2023). Profitable development technology of the Changning-Weiyuan national shale gas demonstration area in the Sichuan Basin and its enlightenment. *Natural Gas Industry B, 10*(1), 73-85. [Crossref]

[10] Li, H. (2022). Research progress on evaluation methods and factors influencing shale brittleness: A review. *Energy Reports, 8*, 4344-4358. [Crossref]

[11] Shizhen, T. A. O., Yiqing, Y. A. N. G., Yue, C. H. E. N., Xiangbai, L. I. U., Wei, Y. A. N. G., Jian, L. I., ... & Jinhua, J. I. A. (2024). Geological conditions, genetic mechanisms and accumulation patterns of helium resources. *Petroleum Exploration and Development, 51*(2), 498-518. [Crossref]

[12] Pu, B., Dong, D., Ning, X., Wang, S., Wang, Y., & Feng, S. (2022). Lithology and sedimentary heterogeneity of Longmaxi shale in the southern Sichuan Basin. *Interpretation, 10*(1), T45-T56. [Crossref]

[13] Luo, T., Guo, X., He, Z., Zhao, J. X., Tao, Z., Dong, T., ... & Chen, J. (2024). Contrasting fracturing and cementation timings during shale gas accumulation and preservation: An example from the Wufeng-Longmaxi shales in the Fuling shale gas field, Sichuan Basin, China. *Marine and Petroleum Geology, 170*, 107138. [Crossref]

[14] He, S., Li, H., Qin, Q., & Long, S. (2021). Influence of mineral compositions on shale pore development of Longmaxi Formation in the Dingshan area, southeastern Sichuan Basin, China. *Energy & Fuels, 35*(13), 10551-10561. [Crossref]

[15] Xusheng, G. U. O., Dongfeng, H. U., Yuping, L., Zhihong, W., Xiangfeng, W., & Zhujiang, L. (2017). Geological factors controlling shale gas enrichment and high production in Fuling shale gas field. *Petroleum Exploration and Development, 44*(4), 513-523. [Crossref]

[16] Fu, H., Huang, L., Hou, B., Weng, D., Guan, B., Zhong, T., & Zhao, Y. (2024). Experimental and numerical investigation on interaction mechanism between hydraulic fracture and natural fracture. *Rock Mechanics and Rock Engineering, 57*(12), 10571-10582. [Crossref]

[17] Gong, X., Jin, Z., Ma, X., Liu, Y., Li, G., & Guo, Y. (2025). Experimental study of the effect of natural fracture curvature on hydraulic fracture propagation behavior. *Scientific Reports, 15*(1), 20716. [Crossref]

[18] Wei, Y., Liu, Q., Lu, S., Zhao, R., Song, Z., & Mou, Y. (2025). Accumulation mechanisms of nonmarine shale oil in China: A case study of the Shahejie Formation in Raoyang Sag, Bohai Bay Basin. *Science China Earth Sciences*, 1-21. [Crossref]

[19] Liu, Y., Zheng, X., Peng, X., Zhang, Y., Chen, H., & He, J. (2022). Influence of natural fractures on propagation of hydraulic fractures in tight reservoirs during hydraulic fracturing. *Marine and Petroleum Geology, 138*, 105505. [Crossref]

[20] Liu, X., Qu, Z., Guo, T., Sun, Y., Wang, Z., & Bakhshi, E. (2019). Numerical simulation of non-planar fracture propagation in multi-cluster fracturing with natural fractures based on Lattice methods. *Engineering Fracture Mechanics, 220*, 106625. [Crossref]



Jing Li received a master's degree in Mineral Prospecting and Exploration from Southwest Petroleum University in 2012. She is currently a senior engineer at Institute of Geological Exploration and Development of CNPC Chuanqing Drilling Engineering Company Limited. Her primary research focuses on shale gas exploration and development. (Email: ljing_dyy@cnpc.com.cn)



Hu Li received a Ph.D. in Geological Resources and Geological Engineering from Southwest Petroleum University in 2020, conducted postdoctoral research at Southwest Petroleum University from June 2021 to May 2024, and is now an Associate Professor and Master's Supervisor at Sichuan University of Science & Engineering. He was listed among the "World's Top 2% Scientists" (Stanford University and Elsevier database) in 2023 and 2024. His research interests are petroleum geology, fracture and fault analysis, shale gas, carbon capture and storage, geomechanics, artificial intelligence, geology, and interdisciplinary studies.

He serves as the Founding Editor-in-Chief of the Journal of Geo-Energy and Environment; Associate Editor of Geoscience Data Journal (SCI), Journal of Petroleum Geology (SCI), and Frontiers in Earth Science (SCI); Academic Editor of PLOS ONE (SCI) and International Journal of Energy Research (SCI); Editorial Board Member of Scientific Reports (SCI), Frontiers in Energy Research (SCI), Geotechnical and Geological Engineering (ESCI, EI), AIMS Geosciences (ESCI), The Scientific World Journal, among others; youth editorial board member and guest editor of more than ten professional journals; and reviewer for over 50 professional journals. He is a distinguished editor with Springer Nature and a distinguished young editorial board member of Advances in Geo-Energy Research. (Email: lihu860628@126.com)